Astron. Astrophys. 293, 252–262 (1995)

ASTRONOMY AND ASTROPHYSICS

Infrared lines as probes of solar magnetic features

X. He I 10830 Å as a diagnostic of chromospheric magnetic fields

I. Rüedi[1], S.K. Solanki[1], and W.C. Livingston[2]

[1] Institute of Astronomy, ETH–Zentrum, CH-8092 Zürich, Switzerland
[2] National Solar Observatory, NOAO*, P.O. Box 26732, Tucson, AZ 85726, USA

Received 11 April 1994 / Accepted 9 May 1994

Abstract. The need for a simple but quantitative diagnostic of upper chromospheric magnetic fields is keenly felt. We develop the He I 10830 Å line as such a diagnostic. An application to observations of an active region allows us to compare the magnetic field in the upper chromosphere with the field in the underlying photosphere. In general, the magnetic field in the chromosphere is found to be significantly more homogeneous. We find that dB/dz in the umbra of a large sunspot (0.4–0.6 G km^{-1}) is similar to other determinations of this quantity over an equivalent height range. Also, dB/dz decreases outwards in the spot. Thus, in the outer penumbra it has dropped to 0.1–0.3 G km^{-1}. A comparison of these values with the results of dB/dz measurements in the photosphere suggests that dB/dz decreases with height. We also find evidence for magnetic canopies near sunspots and for the conservation of magnetic flux with height in solar plages when averaged horizontally over a few arc s. Observations of complex Stokes V profiles at the neutral line in a sunspot penumbra (crossover effect) suggest that the upper chromospheric penumbral magnetic field is not fluted to the same extent as the photospheric field. The large line broadening of He I (up to 10 km s^{-1}) is found to be due to motions which are largely field aligned.

Key words: Sun: magnetic fields, sunspots, chromosphere – techniques: polarimetric

1. Introduction

Magnetic fields dominate the structure and the energetics of the outer solar atmosphere, but in the vast majority of cases they have been measured only in the photosphere. A number of diagnostics do exist for the measurement of chromospheric and low-coronal magnetic fields. Examples are the Ca II 8542 Å, Hα and Hβ lines for the chromosphere (e.g. Giovanelli & Jones 1982; Jones 1985; Wang & Shi 1992; Dara et al. 1993), the C IV emission line for the transition region (e.g. Tandberg-Hanssen et al. 1981; Henze et al. 1982; Hagyard et al. 1983; Henze 1991) and microwave emission from the corona (e.g. Gelfreikh & Lubyshev 1979; Schmahl et al. 1982; Kundu & Alissandrakis 1984; Krüger et al. 1986; Brosius et al. 1992; Lee et al. 1993a,b; Gary & Hurford 1994; see Klein 1992 for a review). The reason most of these diagnostics have been only moderately used, in particular for quantitative studies, is that they are all affected by significant drawbacks, such as the need for satellite observations and moderate Zeeman sensitivity for the C IV lines, the complicated line formation mechanism and splitting pattern, as well as the large line formation height range (Hα, Hβ), or the often low temporal and spatial resolution and sensitivity. Another promising diagnostic, in particular of weak, inclined fields, is the Hanle effect, which has been used to detect magnetic canopies in the lower chromosphere (Faurobert-Scholl 1992, 1994).

In this paper we develop the He I 10830 Å line as a quantitative diagnostic of the magnetic field in the upper chromosphere. This line can overcome most of the problems cited above. It was pioneered as a qualitative magnetic diagnostic by Harvey & Hall (1971), who obtained magnetograms in it. There is also a rich literature on the response of the unpolarized profile of He I 10830 Å to solar activity, i.e. finally to the solar magnetic field (e.g. Namba 1960, 1963; Thompson et al. 1993; Harvey & Livingston 1994; Harvey 1994). We present the first results obtained from Stokes I and V *spectra* observed in active regions and compare them with photospheric measurements. Stokes I signifies unpolarized, Stokes V net circularly polarized light.

Send offprint requests to: I. Rüedi

* Operated by the Association of Universities for Research in Astronomy, Inc. (AURA) under cooperative agreement with the National Science Foundation.

2. The He I 10830 Å line as a magnetic diagnostic

The advantages of the He I 10830 Å line for the measurement of upper chromospheric magnetic fields, are summarized below:

- The He I line can be observed from the ground with normal CCD's or other standard detectors, at a reasonable spatial resolution.
- Avrett et al. (1994) and Fontenla et al. (1993) showed that in standard atmospheric models this line is formed entirely in the upper chromosphere (formation height: 1600 to 2200 km above the quiet sun unit continuum optical depth value $\tau_c = 1$), with no contribution at all from the photosphere, which greatly simplifies its interpretation.
- It is prominent over both sunspots and active region plages, so that the magnetic field throughout active regions can be determined easily down to a limiting strength of roughly 50 G (whereby this value represents the field strength averaged over the spatial resolution element).
- The He I line is in general optically thin or at the most marginally optically thick outside filaments (Giovanelli & Hall 1977; Avrett et al. 1994), so that no complicated radiative transfer calculations or details of the line formation are required for the measurement of the magnetic field.
- Vector polarimetry of this line should be straightforward. In addition – due to its optical thinness – if the four Stokes parameters are measured, then the full magnetic vector can be easily derived.
- Photospheric lines are present in the nearby spectrum, allowing simultaneous and cospatial measurement of the photospheric magnetic field.

Unfortunately, the He I line is not free of disadvantages.

- It has a limited Zeeman sensitivity and does not split sufficiently to allow a direct and model independent measurement of the intrinsic chromospheric magnetic field strength. This may not be such a major disadvantage, since the upper chromospheric field is expected to be relatively homogeneous over a few seconds of arc (but see Sect. 5.6).
- The sensitivity of CCDs and infrared detectors (InSb) at 10830 Å is relatively small.
- The blending between different He I transitions must be taken into account (see below).
- The strength of the He I line is much reduced over less active areas (e.g. Harvey & Livingston 1994), which renders the measurement of the magnetic field outside active regions difficult.

He I has three different transitions near 10830 Å, all from the same lower level having an excitation potential of 19.73 eV, which is populated by recombination (Fontenla et al. 1993; Avrett et al. 1994). The wavelengths λ of these transitions, their effective Landé factors $g_{\rm eff}$ and relative oscillator strengths f are listed in Table 1. The f values have been normalized such that summing over the multiplet $\sum_i f_i = 1$.

We are mainly interested in the two strong components, blended together at 10830.4 Å. Since the line is rarely significantly saturated outside filaments, and never reaches large depths in our observations, this blending does not pose a problem for the analysis. There is a minute water vapor blend coinciding with the wavelength of the two strong components (Giovanelli & Hall 1977), but it is negligible in our observations which were recorded at a time of low water content of the earth's atmosphere. We judged this from the strength of other water vapor lines in the nearby spectrum. A Ca I line at 10829.3 Å ($4p\ ^3F_3^\circ - 6d\ ^3D_2$, $g_{\rm eff} = 1.0$) completely distorts the weakest He I component and slightly affects the blue wing of the strong component at 10830.38 Å . Therefore we place somewhat more weight on the analysis of the line centre and red wing of this component than on its blue wing.

Table 1. Line parameters

Line	λ [Å]	Transition	$g_{\rm eff}$	Relative Osc. Strength f
He I	10828.99	$2s\ ^3S_1 - 2p\ ^3P_0$	2.000	0.111
He I	10830.38	$2s\ ^3S_1 - 2p\ ^3P_1$	1.750	0.333
He I	10830.38	$2s\ ^3S_1 - 2p\ ^3P_2$	0.875	0.556

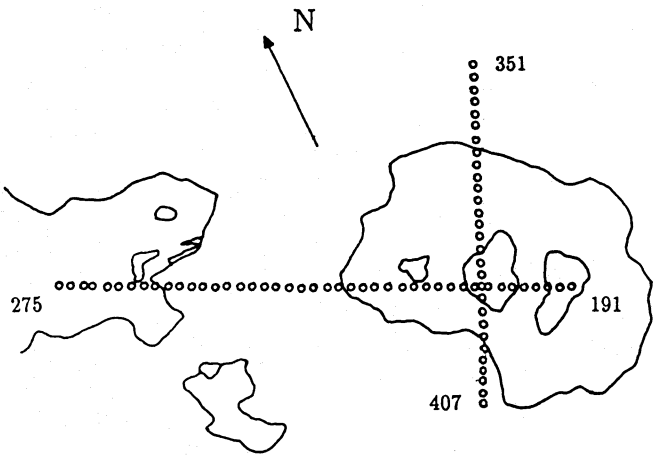

Fig. 1. Umbral and penumbral contours of the analysed active region. The small circles mark the positions at which spectra were obtained. Beginning and end spectrum number are marked

3. Observations

The observations analyzed in this paper were obtained using the McMath-Pierce telescope on Kitt Peak and the main spectrograph with the new infrared grating. The spatial resolution is dominated by seeing and is estimated to be 3″–5″. The spectral resolving power is approximately 180 000. Stokes $I \pm V$ were recorded consecutively at each wavelength. 12 wavelength scans were coadded in order to average out seeing-induced distortions of the spectrum. The rms noise is approximately $10^{-3} I_c$, where I_c is the continuum intensity. Since the spectra are highly oversampled, we enhanced the S/N ratio of the data by Fourier filtering.

The bulk of the observations were carried out on 23rd April 1993 in an active region not too far away from disc centre. They sampled different features such as plage, umbra, penumbra and superpenumbral canopy. Here we restrict ourselves mainly to the discussion of one large active region at ($\mu = \cos\theta \approx 0.94$).

Figure 1 shows the contours of the sunspots of the region as well as the positions at which the spectra were obtained (small circles). The observations were carried out in the order of increasing spectrum number. Note that the different umbrae of the leader spot had different brightnesses. The westernmost one was the darkest.

The covered wavelength range was approximately 10826.0–10831.5 Å, which, in addition to the chromospheric He I 10830 Å line, also contains a photospheric Si I line (λ = 10827.14 Å, transition: $4s\ ^3P_2^\circ - 4p\ ^3P_2$, χ_e = 4.93, g_{eff} = 1.5, log gf=0.53). This log gf value was determined from a fit to a quiet-sun Fourier transform spectrometer (FTS) spectrum obtained by Delbouille et al. (1981).

A sample observation of these two lines in an active region is shown in Fig. 2 (solid curves). Note that the extended red wing of the He I profile is probably not due to a blend, but rather reflects a velocity-induced line shift and asymmetry, since there are spectra in which the spectral line is narrow and symmetric with no absorption at these wavelengths.

Two FTS spectra, recorded in a plage (μ = 0.65) and an umbra (μ = 0.52), enabled us to check some of the results obtained from the above observations by using other, better suited photospheric diagnostic lines. These FTS data, covering the wavelength range 1.03–1.48 μm, are described in detail by Rüedi et al. (1994).

4. Method

4.1. The He I line

The method presented here rests on the fact that we are observing an optically thin line, which, due to its large non-magnetic width, is still in the weak-field regime. Inside filaments the line does become optically thick, however (Harvey & Livingston 1994). The validity of the assumption of a weak field was confirmed with the help of explicit model calculations. The weak-field approximation was found to be an excellent representation for $B \lesssim$ 1500–2000 G. These values are never exceeded in the chromospheric layers of the active region studied here (Sect. 5). This allows us to write $V = \Delta\lambda_H \frac{dI_m}{d\lambda}$, where I_m is the intensity profile produced in the magnetic component of the atmosphere. The Zeeman splitting $\Delta\lambda_H$ is given by $\Delta\lambda_H = 4.67 \times 10^{-13} g_{eff} \lambda^2 B \cos\gamma$, where g_{eff} is the effective Landé factor, λ the wavelength in Å, B the magnetic field strength in G and γ is the angle between the magnetic vector and the line of sight. Assuming a filling factor of 1, i.e. a homogeneous field covering the spatial resolution element of the observation, the scaling factor between the Stokes V profile and the derivative of the observed Stokes I profile delivers the longitudinal magnetic field strength $B\cos\gamma$. Neglecting for the moment that the He I line is a blend of different components, we can write

$$V = 4.67 \times 10^{-13} g_{eff} \lambda^2 B \cos\gamma \frac{dI}{d\lambda}, \quad (1)$$

where I now is the observed Stokes I profile. Due to the optical thinness of the He I line Eq. (1) can be generalized to Stokes Q and U using the second derivative of Stokes I (Stenflo 1985; Solanki et al. 1987; Landi Degl'Innocenti 1992) and the transverse components of the magnetic vector may be obtained if the respective Stokes profiles are observed.

When fitting the observed profiles, we do take into account that the He I profile is composed of multiple components. We first reproduce the observed Stokes I profile by fitting it with a superposition of Voigt profiles weighted with the respective oscillator strengths of the different transitions (Table 1). The synthetic Stokes I profile I_s has the form

$$\frac{I_s(\lambda)}{I_c} = [I_c - h \sum_{j=1}^{n} f_j \phi_j(a, \Delta\lambda_D, \lambda_j)]/I_c, \quad (2)$$

where I_c is the continuum intensity, j runs over the three line components (see Table 1), ϕ_j is a Voigt profile, a its damping constant (a free parameter), $\Delta\lambda_D$ the Doppler width (also a free parameter) and the λ_j are the central wavelengths of the three line components. $\sum_{j=1}^{3} \lambda_j/3$ is a free parameter, but the relative wavelength shifts between the three components are kept fixed. Finally, h is a factor determined by the fit to the observed line depth.

To obtain the Stokes V profile we first multiply each synthetic Stokes I line component by its respective Landé factor and then apply Eq. (1) which gives the Stokes V profile for a single line component. The total Stokes V profile is the sum of these individual components. The synthetic Stokes V profile, V_s, is therefore given by

$$\frac{V_s}{I_c} = 4.67 \times 10^{-13} \frac{B\cos\gamma}{I_c} h \left(\sum_{j=1}^{3} g_{eff,j} f_j \lambda_j^2 \frac{d\phi_j(a, \Delta\lambda_D, \lambda_j)}{d\lambda} \right). \quad (3)$$

The scaling factor between the observed Stokes V profile and this synthetic profile supplies the longitudinal magnetic field strength $B\cos\gamma$. An example of a fit is shown in Fig. 2 (dashed line).

We believe that the main assumption underlying our analysis – homogeneity of the magnetic field over the resolution element – is on the whole reasonable. For example, we expect the field lines of the magnetic elements to have diverged enough by this height so that the field should fill the entire available space (Solanki & Steiner 1990; Solanki et al. 1991). This assumption is supported by the fact that the chromospheric magnetic field is observed to be more homogeneous than the photospheric field (Sect. 5, Harvey & Hall 1971; Giovanelli 1980; Giovanelli & Jones 1982). Nevertheless, some stray light (mainly due to seeing) is inevitably present, particularly in sunspots, so that the quantity actually obtained from Eq. (1) or (3) is $\alpha B\cos\gamma + (1-\alpha) B_s \cos\gamma_s$, where α is the fraction of light coming from within the resolution element and $(1-\alpha)$ is the stray light fraction introduced into the observations. $B_s\cos\gamma_s$ is the longitudinal component of the magnetic field in the solar surface elements from which the stray light is coming. In the

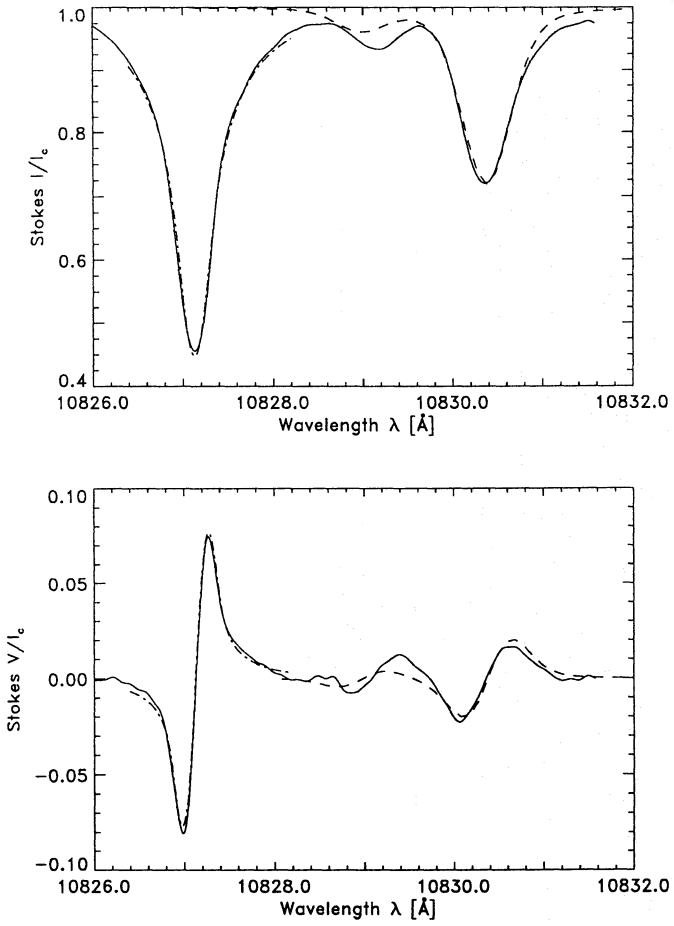

Fig. 2. Measured (solid) and synthetic (dashed and dot-dashed) profiles of umbral Stokes I (upper panel) and Stokes V (lower panel). These profiles correspond to the spectrum numbered 207 in Figs. 1 and 4

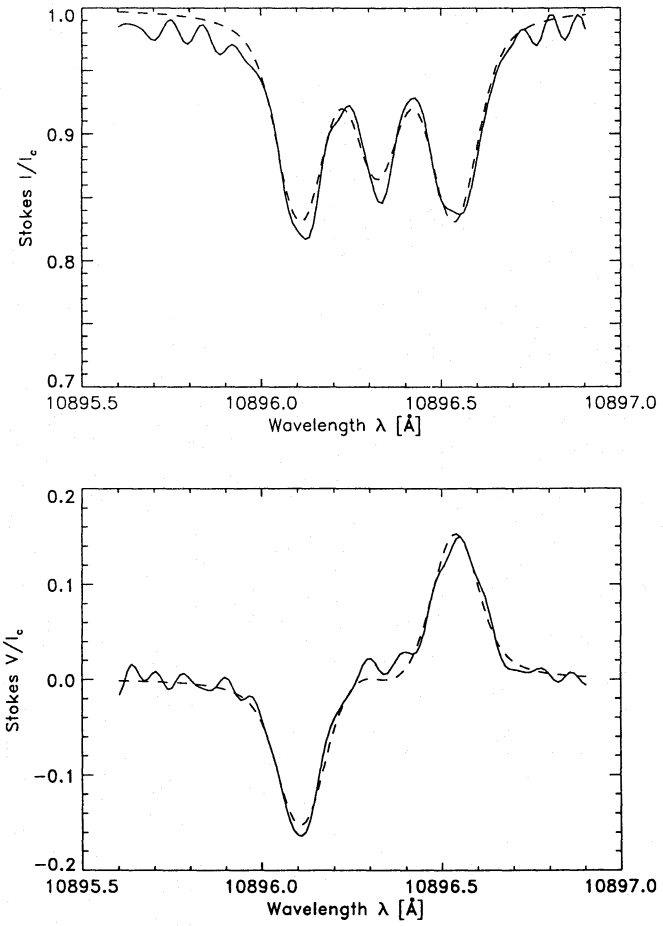

Fig. 3. Measured (solid) and synthetic (dashed) profiles of umbral FTS Stokes I (upper panel) and Stokes V (lower panel) of Fe I 10896 Å

following we assume that $B_s \cos\gamma_s = 0$, i.e. the stray light is non-magnetic.

4.2. The Si I line

In addition to the chromospheric He I line, the simultaneously observed photospheric Si I line was also analyzed in order to compare these two layers. The inversion code described by Solanki et al. (1992, 1994 Papers V and VII of the present series) was used to fit the Si I line. I.e. the observed Stokes I and V profiles of this line were reproduced by carrying out LTE radiative transfer calculations through a two-component model atmosphere composed of a non-magnetic part and a magnetic part. The latter contains a height-independent magnetic field. The non-magnetic component is described by the quiet sun model of Maltby et al. (1986). For the magnetic component model we chose one of the Kurucz (1991) or Maltby et al. (1986) models when fitting spectra observed in sunspots and the Solanki & Brigljević (1992) plage model in the plages. The Si I line is unfortunately not an ideal tool for measuring photospheric fields, since it is insufficiently Zeeman sensitive and relatively temperature-sensitive. The low Zeeman sensitivity is mainly due to the considerable strength and strong saturation of this line, which increases its non-magnetic width to the extent that it is larger than the Zeeman splitting for most photospheric field strengths. Thus the intrinsic field strength B could be determined only for a minority of profiles (mainly in umbrae) and even then only with relatively low accuracy. In the rest of the cases we only obtained $\alpha B \cos\gamma$, i.e. a similar quantity to what we obtained in the chromosphere. In Fig. 2, the best fit to the Si I line is indicated by the dot-dashed curve.

4.3. The Fe I lines

For the FTS spectrum of the umbra we have used the two Landé $g = 1.5$ Zeeman triplets Fe I 10783.07 Å (transition: $c\ ^3P_0 - z\ ^3P_1^\circ$, $\chi_e = 3.11$, $\log gf$=-2.60) and 10896.32 Å (transition: $c\ ^3P_1 - z\ ^3P_2^\circ$, $\chi_e = 3.07$, $\log gf$=-2.73) to accurately measure the photospheric field (recall that $g = 1.5$ at 1.1 μm produces a Zeeman splitting corresponding to that of the $g = 3$ line at 5250 Å). Due to their small non-magnetic width, these lines are completely split, in contrast to the Si I line. The Stokes I and V profiles of Fe I 10896 Å line are plotted in Fig. 3. The field was derived using the inversion code employed earlier to invert the

Si I line. Since these Fe I lines are completely split in sunspot umbrae it is possible to determine B and $\alpha \cos\gamma$ separately.

5. Results

Although we analyzed a number of spatial scans, we concentrate here on the results obtained along the part of the west to east scan shown in Fig. 1. These results are summarized in Fig. 4.

The top panel portrays the spatially averaged longitudinal field strength, $\alpha B \cos\gamma$, as derived from both the He I line (crosses) and the Si I line (diamonds). In the middle panel, the He I line depth (dashed line), as well as its width at half minimum is plotted (solid). Both quantities refer to Stokes I.

The bottom panel shows the intrinsic magnetic field strength B, obtained from the He I line (crosses) and the Si I line (diamonds) in the umbra and in a light bridge, where the Si I line was split by a sufficient amount to allow $\alpha \cos\gamma$ and B to be determined individually. We took this parameter as an indicator of non-magnetic stray light and corrected the helium and silicon values by the same amount even though the helium line is probably less affected by stray light due to the more homogeneous structure of the field at its height of formation. The larger homogeneity of the field in the chromosphere relative to the photosphere is one of the most striking features of the measurements. Whereas the chromospheric $\alpha B \cos\gamma$ changes only by a factor of 4 over the length of the spatial scan, the photospheric $\alpha B \cos\gamma$ varies by a factor of 30. Gaps in the field strength in Fig. 4 are left by spectra to which no reasonable fits with antisymmetric, single component Stokes V profiles could be obtained due to either too small or highly asymmetric observed Stokes V (see Sect. 5.6).

5.1. Umbral magnetic fields

It follows from Fig. 4 that the magnetic field above the umbra is approximately 700–1000 G stronger in the photosphere than in the chromosphere. This difference can be explained by the divergence of the umbral field with height inherent to all MHD models of sunspots (e.g. Pizzo 1986; Jahn 1989). We estimate the height difference between the two layers to be around 1500–2000 km by comparing the line depression contribution function (Magain 1986) of the Si I line with the number density of the He I atoms in the $2s\ ^3S_1$ state given by Avrett et al. (1994). The resulting gradient of the field strength dB/dz lies between 0.35 and 0.67 G km^{-1}, which is in good agreement with gradients determined over a similar or larger height range by other authors (Abdussamatov 1971; Henze et al. 1982; Lee et al. 1993a, b).

The results obtained from the short N-S scan shown in Fig. 1 give similar results. The $\alpha B \cos\gamma$ values are higher by 100–150 G, while dB/dz values are almost identical.

We obtained similar results from the umbral FTS spectrum where the values of $\alpha \cos\gamma$ and B could be determined much more precisely in the photosphere by fitting two better suited Fe I lines (cf. Sect. 4.3). The observed and best-fit profiles of one of these lines are shown in Fig. 3. From this spectrum we derive B = 2580 G in the photosphere and 1830 G in the chromosphere by assuming that the chromospheric stray light is non-magnetic, as in the photosphere, and that $\alpha \cos\gamma$ is the same in both atmospheric layers. The corresponding vertical B gradient is 0.38–0.5 G km^{-1}, in good agreement with the results of the other sunspot, discussed above.

There is a broad light bridge between the two sections of the umbra at the left of Fig. 4 (spectra 197 and 199). In the photospheric layer $\alpha B \cos\gamma$ in the light bridge appears to be reduced relative to the umbrae. In the chromosphere the difference is more significant and of opposite sign: the field strength appears to be higher in the light bridge than in the neighbouring umbra. It is in principle also possible that the field is less inclined in the light bridge than in the neighbouring umbra in the chromospheric layer, but not in the photosphere. Note that in B alone, the light bridge is not visible at the photospheric layer, although this point must be considered open until observations with a more magnetically sensitive line (e.g. Fe I 1.5648 μm) have been carried out.

5.2. Penumbral magnetic fields

In the penumbra $d(\alpha B \cos\gamma)/dz$ is smaller than in the umbra, but this is partly due to the fact that the field becomes increasingly more horizontal near the outer penumbral boundary. We can estimate the intrinsic field strength B at the measured positions in the photospheric layers of the penumbra from values in the literature (see, e.g., the compilation by Solanki & Schmidt 1993). Consequently the ratio of this literature value of $B/B_{\max}$ to the $\alpha B \cos\gamma/B_{\max}$ value obtained from the Si I line gives an estimate of $\alpha \cos\gamma$ in the photosphere. Here $B_{\max}$ is the largest field strength at any location in the sunspot. If we assume that the chromospheric $\alpha \cos\gamma$ value is the same as the $\alpha \cos\gamma$ in the photosphere, then we have obtained an estimate of B in the chromosphere above the penumbra as well. Comparing the photospheric with the chromospheric B values gives $dB/dz \approx$ 0.15–0.35 G km^{-1} in the outer penumbra. This value is smaller than the dB/dz obtained in the umbra. In the inner penumbra the dB/dz is much closer to the umbral value. The large range of possible penumbral dB/dz values reflects uncertainties in the height of formation of the He I line and possible deviations of this sunspot from the standard $B(r)/B_{\max}$ distribution used. Note that in the above procedure we have assumed that $\alpha \cos\gamma$ is the same in the photosphere and the chromosphere. In reality we expect this product to be somewhat larger in the chromosphere. After taking this into account, our best estimate of dB/dz in the outer penumbra becomes 0.1–0.3 G km^{-1}.

The trend of decreasing dB/dz with increasing distance from the centre of the sunspot is in good agreement with the results of Bruls et al. (1994, Paper VIII of the present series), who compared the field strength at two heights in the photosphere. It is also consistent with the trend reported by Lee et al. (1993a), but it is opposite to the result of Abdussamatov (1971) who found a larger dB/dz for smaller B. Although the magnitude of our gradients agrees well with dB/dz derived over a similar height range (e.g. Hagyard et al. 1983), in both the umbra and the

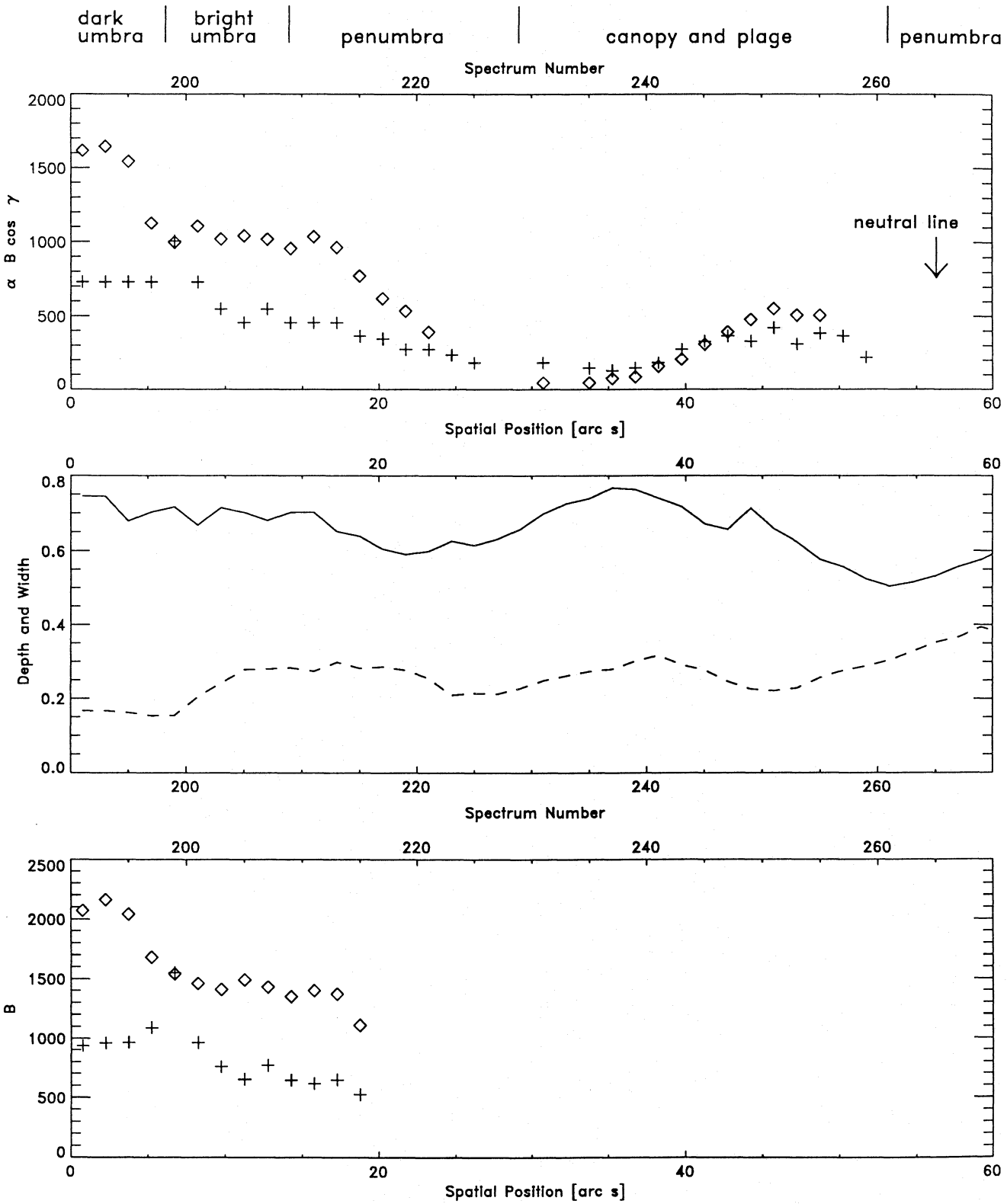

Fig. 4. Top panel: Spatially averaged longitudinal magnetic field strength $\alpha B \cos\gamma$ along the W–E scan shown in Fig. 1 measured in the Si I line (diamonds) and in the He I line (crosses). **Middle panel:** Line depth (dashed) normalized to the continuum intensity, and full width at half minimum in Å (solid) of the He I line. The ordinate scale is valid for both parameters. **Bottom panel:** Intrinsic magnetic field strength B

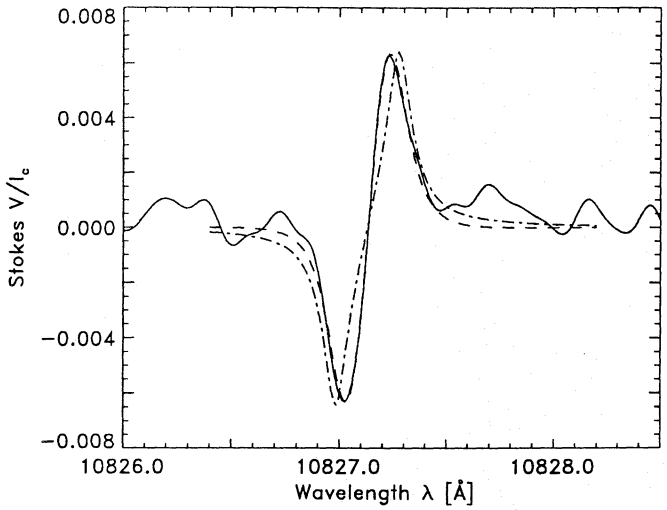

Fig. 5. Measured canopy profile (solid), as well as a fit with a magnetic canopy (dashed) and one with a vertically homogeneous fields of strength 150 G (dot-dashed). Over most of the Stokes V profile the dashed curve is indistinguishable from the solid. This profile corresponds to the Stokes V spectrum numbered 235 in Figs. 1 and 4

penumbra the dB/dz derived here is much smaller than the gradients obtained from purely photospheric lines (Wittmann 1974; Balthasar & Schmidt 1993; Bruls et al. 1994). This comparison suggests that throughout sunspots dB/dz is largest in the photosphere and is considerably smaller in the chromosphere.

5.3. Sunspot canopies

At some positions outside the penumbral boundary the chromospheric $\alpha B \cos\gamma$ is actually larger than the photospheric value (e.g. spectra 235 and 237). These positions are further marked by their proximity to sunspots, small $\alpha B \cos\gamma$ values and Si I Stokes V profiles with particularly narrow peaks and a small peak separation. This is consistent with a superpenumbral magnetic canopy. The fit to such Si I spectra without a magnetic canopy produces Stokes V profiles with too strong wings and too large a peak separation even for very low field strength (see the fit by the dot-dashed curve, B = 150 G, to the solid curve in Fig. 5). Good fits require the presence of a magnetic canopy located roughly 300 km above the unit optical depth, τ_c = 1, surface. Only the core of the Si I line obtains a significant contribution above the canopy base, so that the Stokes V profile formed in the presence of such a canopy is considerably narrower than the Stokes I profile, much of whose width is due to saturation. Such a Stokes V profile (dashed curve in Fig. 5) can reproduce the observations satisfactorily. Thus the shape of the Si I Stokes V profile on its own already suggests the presence of a magnetic canopy surrounding the sunspots. The Stokes V profile shapes of saturated lines may quite generally constitute a new diagnostic of the base heights of magnetic canopies.

In addition, the helium line gives an $\alpha B \cos\gamma$ value consistent with that obtained from the Si I line in the magnetic canopy scenario, but a too large $\alpha B \cos\gamma$ value if the magnetic field seen by Si I is allowed to continue to the bottom of the photosphere (it is these latter values which are plotted in Fig. 4). Consequently, all the evidence points to a low-lying canopy, in good agreement with previous observations of sunspot surroundings based on other diagnostics (Giovanelli 1980; Giovanelli & Jones 1982; Solanki et al. 1992, 1994; Adams et al. 1993).

5.4. Plage magnetic fields

In the plages (cf. spectrum Nos. 241–255) $\alpha B \cos\gamma$ is almost the same at both heights, as expected for spatially unresolved fluxtubes expanding with height and filling all the space at the formation level of the helium line. In other plage regions, located further away from sunspots, we observed an even closer correspondence between the two values, which were of the order of 150 – 300 G. This is also true for the FTS plage spectrum.

The difference between the He I and the Si I $\alpha B \cos\gamma$ found for spectra 249–255 is significant. This is the only example of a plage region in which He I shows a significantly weaker field. One possible explanation of the difference is the interaction between the vertical small flux tubes forming the plage and the almost horizontal field of the superpenumbral canopy – recall that these profiles lie just outside a spot; see Fig. 1. The Si I line has a significant contribution from below the magnetic canopy and mainly detects the vertical flux-tube field which, due to $\cos\gamma \approx 1$, gives a large $\alpha B \cos\gamma$. Higher up the magnetic field of the flux-tubes has merged with the sunspot canopy and has probably been bent to a large degree, thus lowering the $\alpha B \cos\gamma$ visible in the He I line. In any case, we expect the magnetic configuration at such locations to be complex and not easily predictable.

5.5. He I line depth and width

The central frame of Fig. 4 shows the depth and width variations of the helium line along the W–E spatial scan. The plotted line depth $1 - I_l/I_c$ is normalized to the continuum intensity I_c. I_l is the rest intensity in the line core. The variation of the line depth does not appear to be correlated with the magnetic field strength. In particular, the He I line is weakest in the dark part of the sunspot umbra and in the light bridge where the chromospheric field is largest. In addition, the variation of the line depth (it varies by a factor of 2.7 in the plotted region) is slightly smaller than the variation in $\alpha B \cos\gamma$ derived from He I (factor of 3.5 over the figure). The He I line width varies by a factor of 1.6 over the length of the scan.

Interestingly, the Stokes I and V profiles of the He I line are particularly broad there where the Stokes V profile of the Si I line is particularly narrow, i.e. at the location of the superpenumbral canopy. The He I line is also most strongly shifted relative to the Si I profile at these positions. The shift of 300–400 m s^{-1} is consistent with the signal of the inverse Evershed effect seen in the He I line. Outside the sunspot we do not expect the Stokes I profile of Si I to show such a sizable shift caused by the photospheric Evershed effect since this line is mainly formed below the magnetic canopy and the Evershed effect is

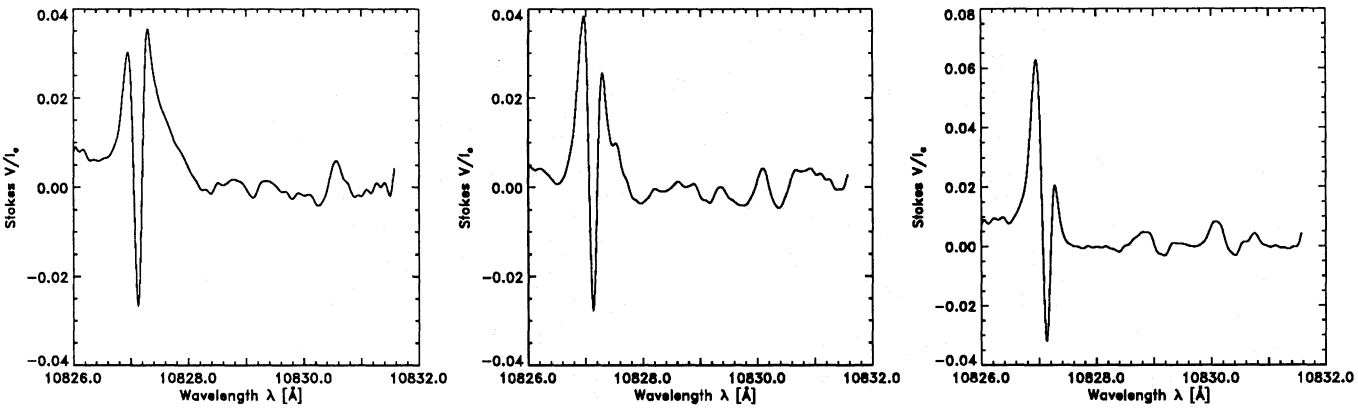

Fig. 6. Complex Si I and He I Stokes V line profiles probably exhibiting the crossover effect. Plotted are the spectra numbered 261, 263 and 265 (from left to right) observed near the apparent neutral line in a sunspot penumbra (see Fig. 4)

only visible above the canopy at such locations (Solanki et al. 1994). We can estimate the broadening velocity by comparing with the He I line width at the neutral line; the line width is smallest at that location (marked by the vertical arrow in Fig. 4) and corresponds to 7.8 km s^{-1}. The largest width that the He I line reaches in the plotted data is 12.9 km s^{-1}, which corresponds to a broadening velocity of 10.3 km s^{-1} relative to the width at the neutral line. This broadening velocity is a lower limit, since the He I line width at the neutral line may partly be due to a velocity broadening as well.

This difference in line width suggests that the major part of the velocity broadening is due to field aligned motions. The large excess broadening velocity may be related to the chromospheric inverse Evershed effect. In this case either there are sizable small-scale velocities that are much larger than the large-scale inverse Evershed flow, or these small-scale velocities are much more inclined to the horizontal (recall that we see no line shifts larger than 300–400 m s^{-1}). In either case, the Evershed effect would be highly inhomogeneous. The other possibility is that the excess broadening velocity is a signature of unresolved waves or oscillations, e.g. running penumbral waves, (Zirin & Stein 1972; Giovanelli 1972; Lites et al. 1982; see review by Lites 1992). Of course, both effects may contribute. The extra broadening is unlikely to be purely thermal, since a line width of 13 km s^{-1} corresponds to a temperature of over 40 000 K. Even the width of the narrowest profile corresponds to T $\approx$ 16 000 K. Thus, if we assume that the He I line is formed at a more nearly 'normal' chromospheric temperature of 6 000–12 000 K, then we find that even at the neutral line the profile is velocity broadened by 4–6 km s^{-1}. This velocity may still be field aligned, even at the neutral line due to the possible presence of uncombed field, i.e. magnetic field with different inclinations in bright and dark penumbral filaments (see Sect. 5.6).

5.6. Complex profile shapes at the neutral line

In the silicon line spectra Nos. 260 to 270, located in the limbward penumbra of the following spot, we observe complex profiles suggestive of the crossover effect (Grigorjev & Katz 1972; Golovko 1974), which is best explained by a combination of magnetic and velocity gradients along the line of sight (e.g. Sánchez Almeida & Lites 1992; Solanki & Montavon 1993). Three such spectra (Nos. 261, 263, 265) are shown in Fig. 6. Before we discuss these profiles further we must first make certain that these strange profile shapes are really solar and not too heavily influenced by the instrument.

In principle, it is possible to produce spectra of this shape through instrumental cross-talk from Stokes Q or U into V (the I to V cross-talk was removed during data reduction). To test the possible importance of cross-talk we calculated the Müller-matrix of the McMath-Pierce telescope for the appropriate times and wavelength assuming unpolutted aluminium mirrors. The largest cross-talk term contributing to Stokes V is found to be from Stokes U and is roughly 20% or less. We can judge the maximum effect of the cross-talk by assuming the worst-case: $\gamma = 90°$, $\chi = 45°$, $U \rightarrow V$ crosstalk of 20% and no non-magnetic stray light. Even under these conditions the maximum Stokes V amplitude produced by the crosstalk is approximately 0.011 (for B=1500 G, a typical field strength in the mid-penumbra), which is below 1/3 the amplitude of the observed Stokes V profiles at and near the neutral line. Thus the observed Stokes V profiles cannot simply be a product of the cross-talk. Could the cross-talk sufficiently distort 'normal' Stokes V profiles observed near the neutral line? To test this we added the worst-case $U \rightarrow V$ cross-talk profile to a normal Stokes V profile, chosen such that the resulting amplitude of the composite Stokes V profile equals the observed Stokes V amplitude. Although the final Stokes V profile can be quite asymmetric (an extreme example is shown in Fig. 7), it never shows the three-lobed structure seen in Fig. 6. We conclude that the observed complex shapes of the Si I Stokes V profiles near the neutral line are mainly due to the solar crossover effect.

What about the He I profile? Although the Stokes I line depth is above normal and its flanks are steep, both of which conditions are conductive to strong Stokes V profiles, the observed Stokes V is small. Its amplitude is 7–9 times weaker than that of the Si I Stokes V profile. This should be compared to the normally observed ratio of 3–4. These weak He I profiles

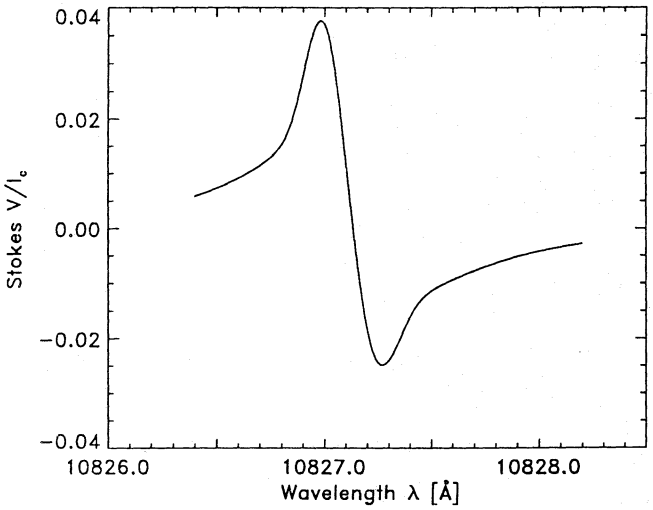

Fig. 7. Most asymmetric synthetic Stokes V profile of the Si I line that can be produced by cross-talk from Stokes U and Q into V

do show the typical signature of the crossover effect, but may, due to their weakness, be more easily affected by cross-talk. On the other hand, the reduced field strength at the chromospheric level means that Stokes U is reduced relative to Stokes V for otherwise the same parameters as in the photosphere. We again tested whether the He I shapes may be strongly affected by cross-talk in a similar manner as we described earlier for the Si I line. The worst case (B = 800–1000G) gives a Stokes V amplitude of 0.0014 produced by $U \rightarrow V$ cross-talk. As in the case of the Si I line, such cross-talk cannot sufficiently distort the observed Stokes V profile. Consequently, the He I line profile also show the crossover effect. Noise, however, begins to become a problem for such weak profiles.

The weakening of the He I Stokes V profile relative to the Si I Stokes V profile already suggests that either the chromospheric magnetic field is more homogeneous than the photospheric, or that the chromospheric velocities are smaller. The observed line width suggests that the latter is not the case, so we conclude that the small-scale inhomogeneity of the penumbral field (uncombed field), which best explains the crossover effect (Solanki & Montavon 1993), is reduced in the upper chromosphere but apparently not absent.

6. Conclusions

We have developed the He I 10830 Å Stokes V profile as a quantitative diagnostic of upper chromospheric magnetic fields and have presented the first results obtained from Stokes I and V profiles of this line. It fills a gap between photospheric magnetic diagnostics and radio observations of the corona.

The results of the present investigation can be summarized as follows:

- The present observations enable us to measure chromospheric magnetic fields down to $\sim$ 100 G, but it should be possible to lower this limit to 50 G or less using observations with a lower noise level.
- The magnetic field distribution at scales larger than 3″ is considerably more homogeneous in the upper chromosphere than in the photosphere. This is consistent with Harvey & Hall's (1971) observation that the magnetic field in the chromosphere is more diffuse than in the photosphere. Nonetheless, the spatially averaged strength of the longitudinal chromospheric magnetic field is found to vary by a larger amount than the He I 10830 Å line depth, at least within the observed active region.
- In plages the magnetic flux through a surface element of 2–3″ in size is equal in the photosphere and chromosphere. This speaks against the presence of significant flux in long low-lying loops (restricted to below the chromosphere) as proposed by Degenhardt & Kneer (1992) to explain the Stokes V asymmetry of photospheric lines (e.g. Solanki & Stenflo 1984). If such loops were common, then the amount of flux seen in the Si I line would be significantly larger than in the He I line, which is not the case in normal plage.
- The vertical magnetic field strength gradients dB/dz we observe in umbrae, 0.35–0.6 G km^{-1}, are compatible with those derived by other authors from comparisons of chromospheric, transition region or coronal with photospheric field strengths (Abdussamatov 1971; Tandberg-Hanssen et al. 1981; Henze et al. 1982; Hagyard et al. 1983; Lee et al. 1993a), but are much smaller than values obtained from the comparison between lines formed at different levels in the photosphere (Wittmann 1974; Balthasar & Schmidt 1993; Bruls et al. 1994).
- The vertical magnetic field strength gradient drops to 0.1–0.3 G km^{-1} in the outer penumbra. This trend is in good agreement with the measurements of Bruls et al. (1994), based on photospheric lines (Hewagama et al. 1993). The value of dB/dz derived here, however, is again much smaller than values measured in the photospheric layers (Bruls et al. 1994; Balthasar & Schmidt 1993). We conclude that the vertical magnetic gradient throughout sunspots, but in particular in the penumbra, is largest in the photosphere and decreases with height. In the penumbra this is consistent with the explanation for the large photospheric gradient given by Solanki & Montavon (1993) and Bruls et al. (1994). In the umbra this behaviour is qualitatively expected from theoretical models.
- The vertical gradient $dB\cos\gamma/dz$ is significantly smaller over a broad light bridge than over the umbra. The light bridge appears to behave like a penumbra in this respect.
- Like the photospheric Si I line, the He I line also exhibits the crossover effect in sunspot penumbrae, at least to within the accuracy of our measurements. The observations suggest that the inclination of the magnetic field in the chromosphere above a sunspot is less inhomogeneous on a small scale than in the photosphere.
- At no location did we find any evidence for an opposite polarity in the chromosphere relative to the underlying photosphere, in contrast to the observations of Dara et al. (1993). If a large-scale inversion of the polarity in the umbra of the

leader spot, such as observed by Dara et al. (1993), were present, our observations would not have failed to show it.

- Considerable mass motions are present in the upper chromosphere above an active region ($\approx$ 10 km s^{-1}). In our observations they express themselves through the enhanced He I line width and Stokes I asymmetry. These motions are mainly field aligned.
- The presence of an almost horizontal magnetic canopy in the upper photosphere near sunspots is confirmed by the comparison of the He I and the neighbouring Si I line. Also, the shape of the Si I Stokes V profile turns out to be a good diagnostic of canopy base heights.
- By extending the technique developed in this paper to the four Stokes parameters, a knowledge of the full magnetic vector in the chromosphere can in principle be achieved. Such measurements would also allow a determination of B without most of the assumptions and uncertainties plaguing the present results. Such observations are planned.

Acknowledgements. We thank J.W. Harvey for putting his code for calculating the Müller matrix of the McMath-Pierce telescope at our disposal and J.O. Stenflo for providing us with the atomic data for the He I triplet.

References

Abdussamatov H.I., 1971, Sol. Phys. 16, 384
Adams M., Solanki S.K., Hagyard M.J., Moore R.L., 1993, Sol. Phys. 148, 201
Avrett E.H., Fontenla J.M., Loeser R., 1994, in Infrared Solar Physics, D. Rabin, J. Jefferies, C.A. Lindsey (Eds.), Kluwer, Dordrecht, IAU Symp. 154, 35
Balthasar H., Schmidt W., 1993, A&A 279, 243
Brosius J.W., Willson R.F., Holman G.D., Schmelz J.T., 1992, ApJ 386, 347
Bruls J.H.M.J., Solanki S.K., Carlsson M., Rutten R.J., 1994, A&A in press (Paper VIII)
Dara H.C., Koutchmy S., Alissandrakis C.E., 1993, A&A 277, 648
Degenhardt D., Kneer F., 1992, A&A 260, 411
Delbouille L., Roland G., Brault J.W., Testerman L., 1981, *Photometric Atlas of the Solar Spectrum from 1850 to 10 000 cm*$^{-1}$, NOAO, Tucson, Az.
Faurobert-Scholl M., 1992, A&A 258, 521
Faurobert-Scholl M., 1994, A&A 285, 655
Fontenla J.M., Avrett E.H., Loeser R., 1993, ApJ 406, 319
Gary D.E., Hurford G.J., 1994, ApJ 420, 903
Gelfreikh G.B., Lubyshev B.I., 1979, Astron. Zh. 56, 562
Giovanelli R.G., 1972, Sol. Phys. 27, 71
Giovanelli R.G., 1980, Sol. Phys. 68, 49
Giovanelli R.G., Hall D.N.B., 1977, Sol. Phys. 52, 211
Giovanelli R.G., Jones H.P., 1982, Sol. Phys. 79, 267
Golovko A.A., 1974, Sol. Phys. 37, 113
Grigorjev V.M., Katz J.M., 1972, Sol. Phys. 22, 119
Hagyard M.J., Teuber D., West E.A., Tandberg-Hanssen E., Henze W., Beckers J.M., Bruner M., Hyder C.L., Woodgate B.E., 1983, Sol. Phys. 84, 13
Harvey J.W., Hall D.N.B., 1971, in Solar Magnetic Fields, R.F. Howard (Ed.), Reidel, Dordrecht, IAU Symp. 43, 279
Harvey J.W., Livingston W.C., 1994, in Infrared Solar Physics, D. Rabin, J. Jefferies, C.A. Lindsey (Eds.), Kluwer, Dordrecht, IAU Symp. 154, 59
Harvey K.L., 1994, in Infrared Solar Physics, D. Rabin, J. Jefferies, C.A. Lindsey (Eds.), Kluwer, Dordrecht, IAU Symp. 154, 71
Henze W., 1991, in Solar Polarimetry, L. November (Ed.), National Solar Obs., Sunspot, NM, p. 16
Henze W., Jr., Tandberg-Hanssen E., Hagyard M.J., Woodgate B.E., Shine R.A., Beckers J.M., Bruner M., Gurman J.B., Hyder C.L., West E.A., 1982, Sol. Phys. 81, 231
Hewagama T., Deming D., Jennings D.E., Osherovich V., Wiedemann G., Zipoy D., Mickey D.L., Garcia H., 1993, ApJS 86, 313
Jahn K., 1989, A&A 222, 264
Jones H.P., 1985, in Chromospheric Diagnostics and Modelling, B.W. Lites (Ed.), National Solar Obs., Sunspot, NM, p. 175
Klein L., 1992, in Methods of Solar and Stellar Magnetic Field Determination, M. Faurobert-Scholl, N. Mein, H. Frisch (Eds.), Obs. de Paris, Meudon, p. 113
Krüger A., Hildebrandt J., Bogod V.M., Korzhavin A.N., Akhmedov Sh.B., Gelfreikh G.B., 1986, Sol. Phys. 105, 111
Kundu M.R., Alissandrakis C.E., 1984, Sol. Phys. 94, 249
Kurucz R.L., 1991a, in Stellar Atmospheres: Beyond Classical Models, L. Crivellari, I. Hubeny, D.G. Hummer (Eds.), Kluwer, Dordrecht, p. 441
Kurucz R.L., 1991b, in Precision Photometry: Astrophysics of the Galaxy, A.G. Davis Philip, A.R. Upgren, K.A. Janes (Eds.), L. Davis Press, Schenectady
Landi Degl'Innocenti E., 1992, in Methods of Solar and Stellar Magnetic Field Determination, M. Faurobert-Scholl, N. Mein, H. Frisch (Eds.), Obs. de Paris, Meudon, p. 7
Lee J.W., Gary D.E., Hurford G.J., 1993a, Sol. Phys. 144, 45
Lee J.W., Hurford G.J., Gary D.E., 1993b, Sol. Phys. 144, 349
Lites B.W., 1992, in Sunspots: Theory and Observations, J.H. Thomas, N.O. Weiss (Eds.), Kluwer, Dordrecht, p. 261
Lites B.W., Chipman E.G., White O.R., 1982, ApJ 253, 376
Magain P., 1986, A&A 163, 135
Maltby P., Avrett E.H., Carlsson M., Kjeldseth-Moe O., Kurucz R.L., Loeser R., 1986, ApJ 306, 284
Namba O., 1960, Ann. d'Astrophys. 23, 902
Namba O., 1963, Bull. Astron. Inst. Netherlands 17, 93
Pizzo V.J., 1986, ApJ 302, 785
Rüedi I., Solanki S.K., Livingston W., Harvey J.W., 1994, A&AS to be submitted
Sánchez Almeida J., Lites B.W., 1992, ApJ 398, 359
Schmahl E.J., Kundu M.R., Strong K.T., Bentley R.D., Smith J.B., Krall J.R., 1982, Sol. Phys. 80, 233
Solanki S.K., Brigljević V., 1992, A&A 262, L29
Solanki S.K., Montavon C.A.P., 1993, A&A 275, 283
Solanki S.K., Schmidt H.U., 1993, A&A 267, 287
Solanki S.K., Steiner O., 1990, A&A 234, 519
Solanki S.K., Stenflo J.O., 1984, A&A 140, 185
Solanki S.K., Keller C., Stenflo J.O., 1987, A&A 188, 183
Solanki S.K., Steiner O., Uitenbroek H., 1991, A&A 250, 220
Solanki S.K., Rüedi I., Livingston W., 1992, A&A 263, 339 (Paper V)
Solanki S.K., Montavon C.A.P., Livingston W., 1994, A&A 283, 221 (Paper VII)
Stenflo J.O., 1985, in Measurements of Solar Vector Magnetic Fields, M.J. Hagyard (Ed.), NASA, Conf. Publ. 2374, p. 263

Tandberg-Hanssen E., Athay R.G., Beckers J.M., Brandt J.C., Bruner E.C., Chapman R.D., Cheng C.C., Gurman J.B., Henze W., Hyder C.L., Michalitsianos A.G., Shine R.A. , Schoolman S.A., Woodgate B.E., 1981, ApJ 244, L127

Thompson W.T., Neupert W.M., Jordan S.D., Jones H., Thomas R.J., Schmieder B., 1993, Sol. Phys. 147, 29

Wang J., Shi Z.,1992, Sol. Phys. 140, 67

Wittmann A.D., 1974, Sol. Phys. 36, 29

Zirin H., Stein A.,1972, ApJ 178, L85

This article was processed by the author using Springer-Verlag TEX A&A macro package 1992.